EPR and ENDOR Studies of 6-Substituted Benzo[a]pyrene Cation Radicals

Paul D. Sullivan,* Ignacio J. Ocasio, Xinhua Chen, and Fouad Bannoura

Contribution from the Department of Chemistry, Ohio University, Athens, Ohio 45701.
Received July 5, 1985

Abstract: The EPR spectrum of 6-methylbenzo[a]pyrene (6-CH_3-BaP) in thallium(III) tris(trifluoroacetate)–trifluoroacetic acid (TTFA/TFA) solutions has been analyzed in terms of the 6-CH_3-BaP cation radical with the aid of the ENDOR spectrum. Benzo[a]pyrene (BaP) in TTFA/TFA gives an EPR and ENDOR spectra which are assigned and analyzed as the 6-(trifluoroacetoxy)benzo[a]pyrene cation radical. The EPR of several other 6-substituted BaP's have been investigated in both H_2SO_4 and TTFA/TFA solutions. Reactions of 6-CH_3-BaP and 6-F-BaP in H_2SO_4 were observed. The EPR spectrum of 6-CH_3-$BaP^{+\cdot}$ changes over a period of an hour into a spectrum identical with that from 6-CH_2OH-$BaP^{+\cdot}$. Similarly, the EPR spectrum of 6-F-$BaP^{+\cdot}$ in H_2SO_4 changes to one identical with 6-OH-$BaP^{+\cdot}$. These observations are discussed in terms of their possible significance to the metabolic reactions of these compounds.

In a recent paper, we reported the interpretation and analysis of the EPR spectrum of the benzo[a]pyrene (BaP) cation radical.[1] In an effort to probe the electronic effects of substituents on the electron densities in the BaP molecule, the cation radicals of several 6-substituted BaP's have been investigated. There is considerable interest in the effects of substituents on polycyclic aromatic hydrocarbons in regard to the metabolism and carcinogenicity of these compounds. Cavalieri and Rogan[2] have recently reviewed the evidence for the involvement of cation radical intermediates in aromatic hydrocarbon carcinogenesis. Considerable circumstantial evidence has been presented particularly with respect to the cation radicals of 6-methylbenzo[a]pyrene (6-CH_3-BaP) and 6-fluorobenzo[a]pyrene (6-F-BaP). In view of this interest in the one-electron oxidation products of substituted benzo[a]pyrenes, it seemed appropriate to investigate in detail the spectroscopic properties of these species.

Experimental Section

BaP was a commercially available sample of high purity (Eastman Kodak), 6-CH_3-BaP and 6-(hydroxymethyl)benzo[a]pyrene (6-CH_2OH-BaP) were prepared by literature methods.[3] Samples of 6-F-BaP, 6-ethylbenzo[a]pyrene (6-CH_3CH_2-BaP), and 6-(methoxymethyl)benzo[a]pyrene (6-CH_3OCH_2-BaP) were kindly provided by Dr. E. Cavalieri. 6-Hydroxybenzo[a]pyrene (6-OH-BaP) was obtained from the National Cancer Institute Chemical Repository.

Cation radicals were prepared by one of two methods: (i) 0.2–0.5 mg of the hydrocarbon were dissolved in 0.2–0.5 mL of 98% H_2SO_4. After approximately 2 min, about 50 μL of the solution was drawn into a capillary tube and placed in the EPR cavity. (ii) A few drops of 0.8 M thallium(III) tris(trifluoroacetate) (TTFA) in trifluoroacetic acid (TFA) were added to a solution of the appropriate hydrocarbon in degassed TFA. Samples were sealed and degassed under vacuum.

EPR spectra were recorded at room temperature (H_2SO_4) or at low temperature, −10 to −35 °C (TFA), in a Varian E-9 EPR spectrometer under various conditions of modulation amplitude and frequency. ENDOR experiments were carried out at the National Biomedical ESR Center, Medical College of Wisconsin, by using a Varian ENDOR spectrometer, with the assistance of Dr. Roger C. Sealy.

The UV–vis spectra were measured on a Hewlett-Packard 8451A diode array spectrometer. HPLC separations were carried out on a Tracor liquid chromatograph by reverse-phase chromatography on a Waters Assoc. μ-Bondpack C_{18} column using gradient elution.

Results

6-Methylbenzo[a]pyrene. Oxidation with either H_2SO_4 or TTFA/TFA led to the production of a well-resolved EPR spectrum. The spectrum from H_2SO_4 oxidation was unstable at room temperature, changing over a period of 2 h from a well-resolved spectrum with a width of ca. 43 G (Figure 1A) to a somewhat narrower (~37 G) less well-resolved spectrum (Figure 1C). The EPR spectrum[4] in TTFA/TFA was, however, found to be relatively stable for several hours at temperatures below 0 °C and had an overall width of ca. 43 G. Although it has been previously shown[4] that BaP and several substituted BaP's (10-CH_3-, 8-F-) undergo reactions in TTFA/TFA which lead to the production of a 6-trifluoroacetoxy cation radical, which is characterized by a smaller overall width than the parent cation radical, this reaction does not appear to occur for 6-CH_3-BaP. When the most reactive positions are blocked from reaction, as shown by 9,10-dimethylanthracene,[5] one can observe a spectrum from the genuine cation radical of the starting material. Analysis of the spectrum in TTFA/TFA was made possible by the observation of an ENDOR spectrum (Figure 2). At −35 °C, nine splitting constants of 0.38, 0.79, 1.68, 1.89, 2.25, 2.52, 3.07, 3.71, and 4.54 G are suggested by the ENDOR spectrum. A large methyl splitting of ca. 7.5 G was also suggested by a weak band around 24 MHz in the ENDOR spectrum. A careful analysis of the wing lines of the EPR spectrum of 6-CH_3-$BaP^{+\cdot}$ followed by many simulations eventually led to an analysis in terms of 10 nonequivalent proton splittings and 3 equivalent methyl proton splittings (Figure 3 and Table I). A comparison with the splittings[1] for $BaP^{+\cdot}$ indicates considerable similarities if the splittings of 6-CH_3-BaP

Table I. EPR Splitting Constants for $BaP^{+\cdot}$, 6-CH_3-$BP^{+\cdot}$, and 6-CF_3CO_2-$BaP^{+\cdot}$

$BaP^{+\cdot}$		6-CH_3-$BaP^{+\cdot}$ (TTFA/TFA)		
splitting[a] const, G	position assigned[a]	EPR splittings (−35 °C)	ENDOR splittings	6-CF_3CO_2-$BaP^{+\cdot}$ ENDOR Splittings
6.63	6	7.38 (CH_3)	~7.5	0.23 (CF_3)
4.57	1	4.45	4.54	4.68
3.77	3	3.63	3.71	3.73
2.95	9	3.06	3.07	2.93
2.75	12	2.47	2.52	2.67
2.23	7	2.21	2.25	2.34
2.11	5	1.81	1.89	1.80
1.94	10	1.70	1.68	1.45
0.82	11	0.79	0.79	1.27
0.54	2	0.44	0.38	0.70
0.37	4	0.34	0.38	0.43
0.19	8			0.23

[a] Reference 1.

(1) Sullivan, P. D.; Bannoura, F.; Daub, G. H. *J. Am. Chem. Soc.* **1985**, *107*, 32–35.
(2) Cavalieri, E.; Rogan, E. *EHP, Environ. Health Perspect.* **1985**, in press.
(3) Dewhurst, F.; Kitchen, D. A. *J. Chem. Soc., Perkin Trans. 1* **1972**, 710–712.
(4) Sullivan, P. D.; Ellis, L. E.; Calle, L. M.; Ocasio, I. J. *Chem. Biol. Interact.* **1982**, *40*, 177–191.
(5) Sullivan, P. D.; Menger, E. M.; Reddoch, A. H.; Paskovich, D. H. *J. Phys. Chem.* **1978**, *82*, 1158–1160.

0002-7863/86/1508-0257$01.50/0

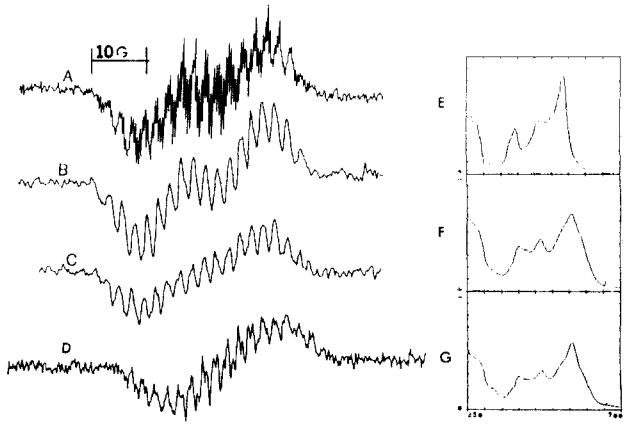

Figure 1. EPR spectra of 6-CH_3-BaP in H_2SO_4 at room temperature: (A) immediately after preparation, (B) 1 h later, (C) 2 h later. Spectrometer conditions, scan time = 8 min, scan range = 80 G, modulation amplitude = 0.2 G, microwave power = 5 mW, time constant = 1 s, gain $\simeq 1 \times 10^5$. D is the EPR spectrum of 6-CH_2OH-BaP in H_2SO_4 under similar spectrometer conditions. Spectra E and F are UV-vis of 6-CH_3-BaP in H_2SO_4 solutions between 250 and 700 nm; spectrum E was recorded immediately after adding H_2SO_4 where spectrum F was recorded 1 h later. Spectrum G is the UV-vis of 6-CH_2OH-BaP in H_2SO_4.

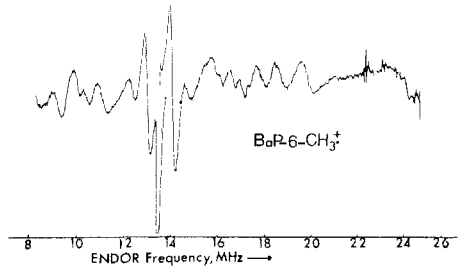

Figure 2. ENDOR spectrum of 6-CH_3BaP in TTFA/TFA at −35 °C.

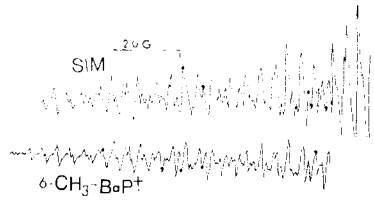

Figure 3. Experimental and simulated (Sim) EPR wing lines of 6-CH_3-BaP in TTFA/TFA at −35 °C. Simulation was done with the EPR splitting constants listed in Table I.

are assigned by analogy with $BaP^{+\cdot}$. The smallest splitting constant is, however, missing, apparently having a value less than the line width (<0.065 G).

The EPR spectral changes of 6-CH_3-BaP in H_2SO_4 (Figure 1A–C) were paralleled by changes in the UV absorption spectra (Figure 1E and F). The major peak at 534 nm shifts to 558 nm within a period of 1 h. The UV spectrum of 6-CH_2OH-BaP in H_2SO_4 taken immediately after dissolution (Figure 1G) was found to be almost identical with the UV spectrum of 6-CH_3-BaP after 1 h (Figure 1F). The EPR spectrum of 6-CH_2OH-BaP in H_2SO_4 immediately after dissolution (Figure 1D) also showed a strong similarity to that of 6-CH_3-BaP after standing for 1 h. It therefore appears that 6-CH_3-BaP reacts in H_2SO_4 to produce the 6-CH_2OH-BaP cation radical. Additionally, the major product formed upon extraction and HPLC separation of a solution of 6-CH_3-BaP in H_2SO_4 after 10-min reaction was found to be 6-CH_2OH-BaP.

6-(Trifluoroacetoxy)benzo[*a*]pyrene. The EPR spectrum observed[6] when BaP is reacted with TTFA/TFA has been attributed to the 6-(trifluoroacetoxy)benzo[*a*]pyrene (6-CF_3CO_2-BaP) cation

(6) Menger, E. M.; Spokane, R. B.; Sullivan, P. D. *Biochem. Biophys. Res. Commun.* **1976**, *71*, 610–616.

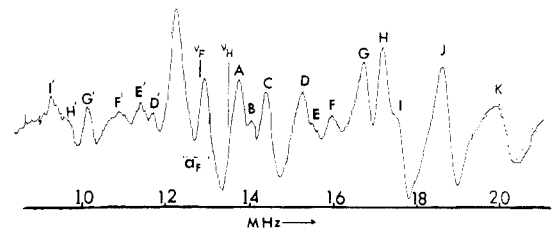

Figure 4. ENDOR spectrum of BaP in TTFA/TFA at −35 °C.

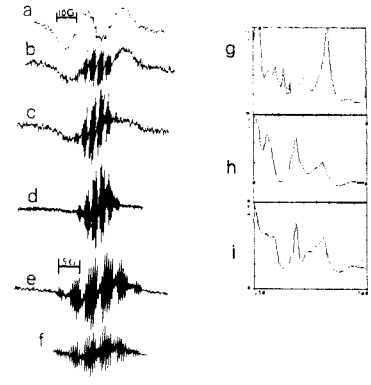

Figure 5. EPR spectra of 6-F-BaP in H_2SO_4 at room temperature: (a) immediately after preparation, (b) 2 h later, (c) 4 h later, (d) 7 h later, (e) 10 h later. Spectrometer conditions were similar to Figure 1 except the scan range is 40 G in e and f. f is the EPR spectrum of 6-OH-BaP in H_2SO_4. Spectrum g is the UV-vis absorption of 6-F-BaP in H_2SO_4 between 250 and 700 nm; h is the same solution after standing for 1 h. Spectrum i is the UV-vis of 6-OH-BaP in H_2SO_4 immediately after dissolution.

radical by analogy with the behavior of anthracene in TTFA/TFA.[5] The trifluoroacetoxylation at the 6-position results in a decrease in the EPR spectral width from 28.8 G in H_2SO_4 to ca. 23.0 G in TTFA/TFA due to the replacement of the proton at the 6-position (splitting 6.63 G) with the three fluorines from the trifluoroacetoxy group. One can estimate the fluorine splittings to be ca. 0.4 G from the decreased width assuming that the sum of the spin densities at the remaining positions remains constant. Further confirmation of the assignment is obtained from the ENDOR spectrum of BaP in TTFA/TFA (Figure 4). A pair of lines on either side of the free fluorine frequency of 12.90 MHz is assigned to three fluorine splittings of 0.23 G. Peaks A–K are thought to be due to the remaining 11 proton splittings. When these values are tabulated (see Table I) and compared to $BaP^{+\cdot}$ and 6-CH_3-$BaP^{+\cdot}$, they are seen to be in good agreement with the values from the other two compounds and the sum of the splitting constants (23.6 G), is in reasonable agreement with the observed width of the EPR spectrum (23.0 G). A simulation of the EPR spectrum of 6-CF_3CO_2-$BaP^{+\cdot}$ has not been achieved to complete the analysis since a sufficiently well-resolved high-intensity EPR spectrum of the wings has not been obtained.

6-Fluorobenzo[*a*]pyrene. The EPR spectrum of 6-F-BaP in H_2SO_4, D_2SO_4, and TTFA/TFA consists of a broad doublet of 17.5 G. On the basis of previous studies with fluorinated naphthalene cation radicals,[7] it is expected that the fluorine splitting should be much larger than the splitting of the proton it is replacing. The large doublet is therefore assigned as the splitting of the fluorine in the 6-position. The spectrum of 6-F-BaP in H_2SO_4 is interesting since it shows a time dependence (Figure 5a–e). Over a period of several hours, the spectrum changes from a broad doublet with little resolution into a much narrower spectrum with considerable resolution. A comparison of the spectrum after 10 h (Figure 5e) with a freshly prepared solution of 6-OH-BaP in H_2SO_4 revealed that the spectra are identical. UV spectral changes further confirmed the similarity. Figure 5g shows the UV spectrum of 6-F-BaP in H_2SO_4 immediately after dissolution, with a strong absorption at 544 nm. After 1 h, the UV spectrum has changed (Figure 5h), the band at 544 nm disappears, and two bands at 524 and 418 nm appear. The UV

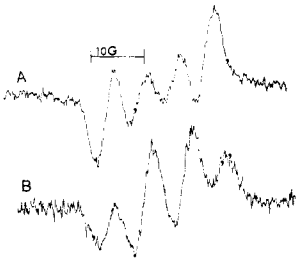

Figure 6. EPR spectra of (A) 6-CH_2OH-BaP and (B) 6-CH_3-BaP in D_2SO_4.

spectrum of 6-OH-BaP in H_2SO_4 is very similar to the latter spectrum, showing bands at 526 and 420 nm (Figure 5i). When the products of the reaction of 6-F-BaP in H_2SO_4 were quenched after a 1 h reaction and extracted into chloroform, followed by evaporation and redissolution in methanol, an HPLC separation then showed the formation of 1,6- and 3,6- and 6,12-BaP quinones, by comparison with known standards.

6-Hydroxybenzo[*a*]pyrene. As noted above, 6-OH-BaP gives a stable well-resolved EPR signal when dissolved in H_2SO_4 (Figure 5f). The EPR spectrum is assumed to be that of the 6-OH-BaP cation radical, and the overall width of 21.7 G is consistent with the substitution of a hydroxyl group for the proton at the 6-position. However, the decrease in width over that of $BaP^{+\cdot}$ is more than anticipated, suggesting that the spin density distribution in the rest of the molecule is changed somewhat by the 6-hydroxyl substituent. The analysis of the complete spectrum is still under investigation and may be possible in the near future.

Other 6-Substituted BaP's. 6-CH_3CH_2-BaP has been reported previously[4] to give a well-resolved EPR signal in both H_2SO_4 and TTFA/TFA. The spectrum has a width of ca. 26.5 G in TTFA/TFA at −35 °C and a width of ca. 28 G in H_2SO_4 at 22 °C. If one assumes that the sum of the spin densities at the protonated positions is the same in 6-CH_3CH_2-$BaP^{+\cdot}$ as in 6-CH_3-$BaP^{+\cdot}$ (i.e., 20.9 G from Table I), then the remaining width in 6-CH_3CH_2-$BaP^{+\cdot}$ should be due to the two β-ethyl protons (assuming the γ-ethyl protons to be negligible). This leads to values of 2.8 G in TTFA/TFA at −35 °C and 3.55 G in H_2SO_4 at 22 °C. These values provide an insight into the conformation of the ethyl group as discussed below. EPR spectra of 6-CH_2OH-BaP and 6-CH_3OCH_2-BaP in H_2SO_4 are very similar to each other as are the spectra in D_2SO_4. The spectrum of 6-CH_2OH-BaP in H_2SO_4 is shown in Figure 1D and is characterized by a width of 37–38 G with poor overall resolution. In D_2SO_4, four broad lines are observed (Figure 6A) which may be due to two large splittings of 13.0 and 6.0 G. The latter can be compared with the expected 1:3:3:1 pattern from the methyl protons when 6-CH_3-BaP is dissolved in D_2SO_4 (Figure 6B).

Discussion

Conformation of 6-CH_3CH_2-$BaP^{+\cdot}$ and 6-CH_2OH-$BaP^{+\cdot}$. It is known[8] that the splitting of a β-proton is dependent on the dihedral angle, θ, between the C–H bond axis and the z axis of the p_z orbital on the adjacent carbon atom (eq. 1). B_0 is usually

$$a_\beta^H = (B_0 + B_2 \cos^2 \theta)\rho_c^\pi \qquad (1)$$

small and can be neglected. For a freely rotating methyl group, the time-averaged value of $\cos^2 \theta$ is $^1/_2$, and, therefore, for 6-CH_3-BaP, if a_β^H = 7.38 G and ρ_c^π = 0.237,[1] then B_2 must equal 62.3 G. The estimated splitting of the β-ethyl protons at −35 °C is 2.8 G which indicates that the preferred conformation of the ethyl group is one in which the dihedral angle of the CH_2 protons is 60° (Fig. 7a). The ratio of β-proton splittings in 6-CH_3- and 6-CH_3CH_2-BaP in TTFA/TFA at −35 °C, 7.38/2.9 = 2.54, is very similar to the same ratio for hexamethylbenzene and hexaethylbenzene cation radicals,[9] 6.63/2.64 = 2.47, in which the ethyl group adopts a similar preferred conformation. The increased

Figure 7. Possible conformation of 6-CH_3CH_2-BaP (a) and 6-CH_2OH-BaP or 6-CH_3OCH_2-BaP (b).

value of the β-ethyl proton splitting in H_2SO_4 at +22 °C is at least partially due to the expected positive temperature dependence of the β-ethyl proton splittings.[10] However, there may also be a contribution from small differences in the spin density distributions between TTFA/TFA and H_2SO_4 solutions. Biologically, 6-CH_3CH_2-BaP is found to be inactive as a carcinogen[11] or mutagen;[12] the out-of-plane position of the CH_3 group which probably persists in the neutral species may provide a steric barrier which prevents or decreases binding of 6-CH_3CH_2-BaP to activating enzymes such as cytochrome P-450. Alternatively, the biological inactivity may simply be due to changes in metabolism between methyl and ethyl substituents.

The apparent inequivalence of the β-protons in 6-CH_2OH-$BaP^{+\cdot}$ (i.e., 13.0 and 6.0 G) and 6-CH_3OCH_2-$BaP^{+\cdot}$ may indicate a preferred conformation for these compounds in which the dihedral angle of the OR group is 30° (Figure 7b). This would provide less of a steric barrier to interaction with activating enzymes and would be consistent with the ability of these compounds to bind to cytochrome P-450.[13]

Spin Density Distribution in 6-CH_3-$BaP^{+\cdot}$ and 6-CF_3CO_2-$BaP^{+\cdot}$. The assignments of the splitting constants in Table I for 6-CH_3-$BaP^{+\cdot}$ and 6-CF_3CO_2-$BaP^{+\cdot}$ were made by analogy with those for the unsubstituted parent compound.[1] The values appear to be eminently reasonable when assigned in this manner and would indicate that the spin density distribution in the rest of the molecule is little changed by substitution at the 6-position with CH_3 or CF_3CO_2. Further attempts to justify these assignments will be made by using other mono- and dimethylated BaP's. If the assignments are borne out, the results would be significant to the metabolism of 6-CH_3-BaP in that they would suggest that changes in metabolic pathways between BaP and 6-CH_3-BaP are likely to be unaffected by electronic factors. Differences most likely arise because of the steric effects of the methyl group and the possible reaction pathways involving oxidation of the CH_3 group.

Reactions in TTFA/TFA. Oxidations in TTFA/TFA have been studied by several groups[5,14-17] and three major reactions have been observed: (i) nuclear substitution, (ii) biaryl coupling, and (iii) side-chain substitution. The one-electron pathway for these reactions competes with a simultaneous two-electron pathway, however, in the case of aromatic hydrocarbons the one-electron intermediate is sufficiently stable in many cases to be observed by EPR spectroscopy. We have previously shown that this is not the case for anthracene which undergoes substitution and further oxidation at the 9- and 10-positions, resulting in the observation of EPR signals from the 9-(trifluoroacetoxy)- and 9,10-(ditrifluoroacetoxy)anthracene cation radicals.[5] It was also noted that when the 9- and/or 10-positions were substituted with methyl groups, substitution was retarded at that position. The reactions

(7) Thomson, D.; MacCulloch, W. J. *Mol. Phys.* **1970**, *19*, 817–832.
(8) Heller, C.; McConnell, H. M. *J. Chem. Phys.* **1960**, 32, 1535–1539.
(9) Carter, M. K.; Vincow, G. *J. Chem. Phys.* **1967**, *47*, 302–312.
(10) Sullivan, P. D.; Menger, E. M. *Adv. Magn. Reson.* **1977**, *9*, 1–48.
(11) Cavalieri, E.; Rogan, E.; Roth, R. "Free Radicals and Cancer"; Floyd, R. A., Ed.; Marcel Dekker: New York, 1982; pp 117–158.
(12) Sullivan, P. D.; Calle, L. M.; Ocasio, I. J.; Kittle, J. D.; Ellis, L. E. "Polynuclear Aromatic Hydrocarbons: Chemistry and Biological Effects"; Bjorseth, A., Dennis, A. J., Eds.; Battelle Press: Columbus, OH, 1980; pp 163–175.
(13) Bayless, J. H.; Sullivan, P. D.; Roach, S. M.; Jablonski, J. *Biochem. Pharmacol.*, in press.
(14) Taylor, E. C.; McKillop, A. *Acc. Chem. Res.* **1970**, *3*, 338–346.
(15) McKillop, A.; Turrell, A. G.; Young, D. W.; Taylor, E. C. *J. Am. Chem. Soc.* **1980**, *102*, 6504–6512.
(16) Elson, I. H.; Kochi, J. K. *J. Am. Chem. Soc.* **1973**, *95*, 5060–5062.
(17) Lau, W.; Kochi, J. K. *J. Am. Chem. Soc.* **1984**, *106*, 7100–7112.

of BaP and 6-CH_3-BaP as reported above are seen to parallel the behavior of anthracene. The observed cation radical from BaP is found to be the 6-CF_3CO_2-BaP cation radical formed most probably by the following sequence of steps (eq 2). The ap-

$$\text{BaP} \xrightarrow{-1e^-} \text{BaP}^{+\cdot} \xrightarrow[-e^-]{CF_3CO_2^-} \text{6-}CF_3CO_2\text{-BaP} \xrightarrow{-1e^-} \text{6-}CF_3CO_2\text{-BaP}^{+\cdot} \quad (2)$$

pearance of a single major product in the HPLC separation of the reaction products,[4] due to the 6-(trifluoroacetoxy)benzo[*a*]-pyrene, is further proof of the identity of the observed cation radical. A similar reaction pathway has been previously proposed[18] for the reaction of BaP with manganic acetate in acetic acid in which the major product is 6-acetoxybenzo[*a*]pyrene.

6-CH_3-BaP is much less reactive in TTFA/TFA; the substitution of the methyl group in the position of highest electron density considerably retards the substitution reactions, the one-electron oxidation product of 6-CH_3-BaP being relatively stable for several hours at reduced temperatures. Reaction is not, however, completely elminated; the 6-CH_3-$BaP^{+\cdot}$ EPR spectrum decays appreciably at room temperature, and a variety of reaction products consistent with both methyl and ring substitution by trifluoroacetoxy groups are found.[4] These results again parallel the behavior seen by 6-CH_3-BaP in manganic acetate–acetic acid mixtures.[18]

Reactions in H_2SO_4. The reactions of 6-CH_3-BaP and 6-F-BaP observed in H_2SO_4 may be of some significance to proposed metabolic pathways for these compounds. Cavalieri[2] has proposed that cation radicals can be generated from polycyclic hydrocarbons by one-electron oxidation with a Fe(V) form of cytochrome P-450. That such a reaction could occur is evidenced by the one-electron oxidation of methylarenes with tris(phenanthroline)iron(III) complexes in TFA.[19] It was further proposed that the cation radicals would then react with nucleophiles, including DNA, at the positions of highest charge density. The metabolic formation of quinones[2,20] from 6-F-BaP is hypothesized to proceed via a cation radical intermediate which is then attacked by a nucleophilic oxygen atom. Adducts of 6-F-BaP to DNA in model systems have also been identified which are consistent with the reaction at the 6-position of BaP. Circumstantial evidence for the intermediacy of cation radicals in the metabolism of 6-CH_3-BaP comes from the identification of adducts in a variety of systems in which the BaP-6-CH_2 group is bound to the 2-amino group of guanine,[21] and the formation of 6-CH_2OH-BaP as a major product of metabolism.[22]

Our studies seem to have demonstrated rather directly that the formation of a cation radicals from 6-CH_3-BaP and 6-F-BaP could lead to the observed reaction products. In H_2SO_4, the first produced one-electron oxidation products appear to react with residual water to give 6-CH_2OH-$BaP^{+\cdot}$ and 6-OH-$BaP^{+\cdot}$, the former yielding 6-CH_2OH-BaP on workup and the latter autoxidizing on workup to give the three benzo[*a*]pyrenequinones (1,6-, 3,6-, and 6,12-).

Acknowledgment. This work was supported by Grant CA-34966 awarded by the National Cancer Institute, DHEW, to P.D.S. We also thank Dr. R. Sealy of the National Biomedical ESR Center at the Medical College of Wisconsin for help in obtaining the ENDOR measurements (supported by National Institutes of Health Grant RR-01008).

(18) Rogan, E.; Roth, R.; Cavalieri, E. "Polynuclear Aromatic Hydrocarbons: Chemistry and Biological Effects"; Bjorseth, A., Dennis, A. J., Eds.; Battelle Press: Columbus, OH, 1980; pp 259–266.

(19) Schlesener, C. J.; Amatore, C.; Kochi, J. K. *J. Am. Chem. Soc.* **1984**, *106*, 3567–3577.

(20) Cavalieri, E.; Cremonesi, P.; Warner, C.; Tibbels, S.; Rogan, E. *Proc. Am. Assoc. Cancer Res.* **1984**, *25*, 124.

(21) Rogan, E. G.; Hakam, A.; Cavalieri, E. L. *Chem.-Biol. Interact.* **1983**, *47*, 111–122.

(22) Hammerik, K. L.; Chiu, P.-L.; Chou, M. W.; Fu, P. P.; Yang, S. K. "Polynuclear Aromatic Hydrocarbons: Formation, Metabolism and Measurements"; Cooke, M., Dennis, A. J., Eds.; Battelle Press: Columbus, OH, 1983; pp 583–597.

A Theoretical Survey of Singly Bonded Silicon Compounds. Comparison of the Structures and Bond Energies of Silyl and Methyl Derivatives

Brian T. Luke,[1a] John A. Pople,[1a] Mary-Beth Krogh-Jespersen,[1b] Yitzhak Apeloig,[1c] Jayaraman Chandrasekhar,[1d] and Paul von Ragué Schleyer*[1d]

Contribution from the Department of Chemistry, Carnegie-Mellon University, Pittsburgh, Pennsylvania 15213, Department of Chemistry, Pace University, New York, New York 10038, Department of Chemistry, Technion-Israel Institute of Technology, 32000 Haifa, Israel, and Institutut für Organische Chemie der Friedrich-Alexander-Universität Erlangen-Nürnberg, D-8520 Erlangen, Federal Republic of Germany. *Received July 5, 1984*

Abstract: The silicon hydrides, SiH_n (n = 1–4), and the entire set of H_3SiX (X = Li, BeH, BH_2, CH_3, NH_2, OH, F and Na, MgH, AlH_2, SiH_3, PH_2, SH, Cl) molecules have been investigated by using ab initio methods. All structural parameters were optimized by use of the 3-21G and 3-21G(*) basis sets. The silyl derivatives are compared with the corresponding methyl compounds. In most cases, the equilibrium geometries of the methyl and silyl molecules are similar. The most notable exception is in silylamine, where a planar geometry is found about the nitrogen. Addition of *d*-functions to the second-row atoms results in a decrease in the bond lengths. The relative H_3Si–X and H_3C–X bond energies depend principally on the electronegativity of the group X. Since SiH_3 has a higher electron affinity and a lower ionization potential than CH_3, groups which are very electronegative or very electropositive have stronger bonds to silicon than carbon.

Silicon, although a contiguous group 4 (group 14 in the more recent notation) element,[1f] often frustrates chemists in their search for analogues of carbon compounds.[2,3] Difficulties in studying many silicon singly bonded species are often attributed to the

0002-7863/86/1508-0260$01.50/0